X-ray absorption and diffraction studies of the mixed-phase state of (Cr_{x}V_{1-x})_{2}O_{3}

D. M. Pease, A. I. Frenkel, V. Krayzman, T. Huang, P. Shanthakumar, J. I. Budnick, P. Metcalf, F. A. Chudnovsky, and E. A. Stern

Phys. Rev. B **83**, 085105 — Published 18 February 2011

DOI: 10.1103/PhysRevB.83.085105

X-ray absorption and diffraction studies of the mixed phase state of $(Cr_xV_{1-x})_2O_3$

D. M. Pease,[a*] A. I. Frenkel,[b†] V. Krayzman,[c,d‡] T. Huang,[a] P. Shanthakumar,[a] J. I. Budnick,[a] P. Metcalf,[e] F. A. Chudnovsky,[f] E. A. Stern[g]

[a]*Department of Physics, University of Connecticut, Storrs, Connecticut 06269 USA*

[b]*Department of Physics, Yeshiva University, New York, New York 10016 USA*

[c]*Ceramics Division, National Institute of Standards and Technology, Gaithersburg, Maryland 20899 USA*

[d]*Department of Materials Science and Engineering, University of Maryland, College Park, Maryland 20742 USA*

[e]*Department of Materials Engineering, Purdue University, West Lafayette, Indiana 47907 USA*

[f]*Ioffe Physico-Technical Institute, St. Petersburg, Russia*

[g]*Department of Physics, Box 351560, University of Washington, Seattle, Washington 98195 USA*

Abstract

X-ray diffraction (XRD) and vanadium X-ray absorption near edge structure (XANES) data have been obtained for $(V_{1-x}Cr_x)_2O_3$ samples containing several concentrations of Cr, crossing the metal-insulator transition (MIT) boundary. For single phase single crystal samples our theoretical results are generally in good qualitative agreement with our experimental single crystal XANES, for both crystal orientations relative to the incident beam electric vector. However, an anomalous peak occurs for both orientations in the *K* pre-edge of the single crystal sample containing 1.2% Cr, a paramagnetic insulator (PI) sample which is in the concentration regime corresponding to the room temperature two phase (coexistence) region of the phase diagram. Upon raising the temperature of 0.4% Cr powdered material to 400 K so that one enters the two phase region of the phase diagram, a similar peak appears and then diminishes at 600 K. These results, as well as experiments done by others involving room temperature and low temperature XANES of a 1.1% Cr sample, suggest that this feature in the V pre-edge structure is associated with the appearance under some circumstances of a small amount of highly distorted VO_6 octahedra in the interface region between coexisting metal and insulating phases. Finally, we find that, for the two phase

* Corresponding author. Electronic address: pease@ims.uconn.edu
† Corresponding author. Electronic address: anatoly.frenkel@yu.edu
‡ Corresponding author. Electronic address: victor.krayzman@nist.gov

regime, the concentration ratio of metal to insulating phase varies between different regions from a sample batch of uniform composition made by the skull melting method.

I. INTRODUCTION

The metal-insulator transition (MIT) in Cr-doped V_2O_3, from paramagnetic metal (PM) to paramagnetic insulator (PI) at room temperature, has attracted much attention since it was discovered.[1] This interest is partly because both PM and PI phases were predicted to be metallic by band structure calculations.[2,3] V_2O_3 is a corundum structure paramagnetic metal (PM) at room temperature and converts to a monoclinic antiferromagnetic insulator (AFI) when cooled to 155 K. On the other hand, the system $(Cr_xV_{1-x})_2O_3$, which converts from the PM state to the PI state at $x \approx 0.01$ maintains a corundum structure through the MIT.[1] In recent years, there have been significant theoretical and experimental advances in our understanding of this system. Held *et al.*[3] applied the local density approximation—dynamical mean field theory (LDA+ DMFT) approach to the $(Cr_xV_{1-x})_2O_3$ system. These authors first applied the LDA to both pure V_2O_3 and $(Cr_xV_{1-x})_2O_3$ with $x = 0.038$. Using the LDA alone, both compositions were calculated to be metallic, a result that disagrees with experiment and is consistent with earlier calculations of Mattheiss.[2] In order to apply the full LDA + DMFT, Held *et al.*[3] then adjusted U, the Mott – Hubbard Coulomb interaction parameter, to obtain a reasonable splitting within the t_{2g} bands. The critical value for splitting of these levels comes out to be about 5 eV. For U values of 4.5 eV, corresponding to a system in the PM phase on the threshold of transforming to the PI phase, the system is metallic. Furthermore, in the occupied states near the Fermi level this system is predicted to show a pronounced peak in the quasiparticle spectrum. Mo *et al.*,[4] using bulk sensitive, high energy photoemission as a probe, subsequently observed such a peak in the occupied density of states in metallic V_2O_3. This peak was observed somewhat above the transition temperature for transformation to the antiferromagnetic insulator (AFI) state.[4] Similar high energy photoemission experiments were then carried out for $(Cr_xV_{1-x})_2O_3$.[5] In agreement with theory, the quasi particle peak detected for metallic V_2O_3 disappears for PI phase material. However, for both the PI and AFI phases, the vanadium 3*d* parts of the photoemission spectra are not simple one peak structures, and there is not a good theoretical understanding of these features.[5] In a recent investigation, Rodolakis *et al.*[6] have measured powder V *K* edge X-ray absorption near edge spectra (XANES) on $(Cr_xV_{1-x})_2O_3$ for *x* corresponding to 1.1% and 2.8% Cr concentrations. These experiments were conducted as a function of temperature and pressure and

compare well to their theoretical calculations for the first and second pre-edge peaks. The authors also find that at edge energy of about 5472 eV there is an enhanced intensity region for the sample with Cr composition 1.1% in the PI regime of the phase diagram, but not in the lower temperature PM regime. For the interpretation of this effect the authors refer to Gougassis *et al.*[7] who discuss the K edge XANES of NiO in terms of a theory involving non local excitations. Rodolakis *et al.*[6] go on to demonstrate that the electronic properties of $(Cr_xV_{1-x})_2O_3$ can vary depending on the (pressure, concentration, temperature) route across the metal insulator transition (MIT) boundary, and that the metallic phase reached by increasing pressure is different than a metallic phase obtained by changing doping or temperature.

The two phase (coexistence) regime of the $(Cr_xV_{1-x})_2O_3$ system is of current interest. The existence of a two phase region, containing both insulating and conducting phases, was reported by McWhan and Remeika in 1970,[1] based on powder X-ray diffraction (XRD) obtained at room temperature. By measuring relative peak intensities McWhan and Remeika[1] obtained a dependence of the ratio of insulating (I) to conducting (M) phase on the concentration of Cr within the coexistence region at room temperature. For their conditions of sample preparation and thermal history, McWhan and Remeika[1] found that at room temperature a sample containing approximately 1% Cr would be PI, but would also contain mixed M and I phases. Based on these early results and interpretation, one infers that the PI nature of such a sample may be due to the fact that the majority I phase prevents the minority M phase from spanning the sample so that a percolating metallic state cannot form. McWhan and Remeika[1] also found in a separate experiment that the room temperature ratio of I to M phases within the coexistence concentration range can depend quite sensitively on the details of thermal history.

Subsequent to the earlier studies by McWhan and Remeika,[1] Jayaraman *et al.*[8] performed temperature dependent powder XRD of $(Cr_xV_{1-x})_2O_3$ with $x = 0.006$, monitoring the (300) peak of the corundum structure. Only the M phase (300) peak was observed at room temperature, and only the I phase peak was observed at 503 K.[8] However, as the temperature was increased through the intermediate temperature coexistence regime, it was observed that the M peak systematically shifted toward the lower angle position of the (300) I peak so that at 473 K the M peak became a shoulder on the I phase peak. These authors attributed this effect to different thermal expansion coefficients between the conducting and insulating phases. To our knowledge,

this explanation of the peak shift of the M peak toward I phase peak as the concentration of M phase decreases has not been tested experimentally.

In a recent theoretical study, Park *et al.*[9] applied cluster dynamical mean field theory to the Mott transition. For their single site calculation they derive a phase diagram that they remark "strongly resembles the phase diagram of Cr doped V_2O_3." This phase diagram is divided up into five regions: bad metal, bad insulator, Fermi liquid, paramagnetic insulator, and the coexistence (two phase) region. For their plaquette calculation, the metallic state in the coexistence region differs from that in the pure Fermi liquid region in featuring a quasiparticle peak that is broadened because of incoherence. The insulating state in the coexistence region has a smaller gap and differences in spectral characteristics relative to the case of a fully developed Mott insulator. For our purposes, the message of this recent calculation is that the electronic structure of $(Cr_xV_{1-x})_2O_3$ in the coexistence regime may be quite different than for the single phase region. Hereafter we will refer to the phase diagram developed by Kuwamoto *et al.*,[10] that takes the hysteresis of this system, upon heating and cooling, into account, and includes the two phase regime.

Previous calculations involving V *K* edge XANES in systems related to $(Cr_xV_{1-x})_2O_3$ have been carried out by Meneghini *et al.*,[11] Joly *et al.*,[12] Cuozzo *et al.*,[13] and Rodolakis *et al.*[6] The calculations of Meneghini *et al.*[11] were devoted to a–b plane dichroism in the AFI phase. The calculations of Joly *et al.*[12] pertained to resonant X-ray scattering experiments in AFI V_2O_3. Cuozzo *et al.*[13] calculated the V *K* edge absorption spectra of V_2O_3 using an eleven atom cluster. This last calculation does not distinguish between polarization directions in a single crystal XANES experiment. The calculation by Rodolakis *et al.*[6] also concentrates on random powders and, for that reason, it does not offer results that differentiate between single crystal orientations relative to the incident beam electric vector.

In the present study, we performed powder XRD studies on $(Cr_xV_{1-x})_2O_3$, made by skull melting[14] and have found that for samples in the two phase concentration regime, the ratio of M to I phase varies between different crystal samples of the same composition. We have also investigated the V *K* edge XANES for single crystal and powder samples as a function of concentration *x* at room temperature as well as for specific concentrations of powder samples as a function of temperature. We have found that there is a pronounced peak C in the V K edge

single crystal XANES of the material with $x = 0.012$, a composition which at room temperature is two phase. Our theoretical results are in reasonable agreement with our experiments for both crystal orientations for the single phase materials, but not for peak C in the two phase sample. This situation is similar to that reported by Rodolakis *et al.*[6] We have measured the region of peak C for other concentrations than investigated in Ref. 6, and have found that peak C is absent both for pure single phase metallic and single phase insulator material, implying peak C has to do with the coexistence of two phases.[1]

The paper is organized as follows. Chapter II describes details about the preparation and characterization of the samples, and a brief description of the computational methods used. Results are presented in Chapter III. Discussion is given in Chapter IV. Summary and Conclusions are presented in Chapter V.

II. EXPERIMENTAL AND COMPUTATIONAL METHODS

Single crystals of $(Cr_xV_{1-x})_2O_3$ with $x = 0$, 0.004, 0.012, 0.029, and 0.052 were prepared by the skull melting technique at Purdue University.[14] In addition, a single crystal sample of pure V_2O_3, thin enough (15 μm) for transmission XANES, was manufactured and used for our pure V_2O_3 results.[15] The samples containing Cr were stoichiometric single crystals of high quality which was confirmed by resistivity measurements, scanning electron microscopy, and XRD. In the pure V_2O_3, this was evident by resistivity measurements: 1) the resistivity dropped by 7 orders of magnitude above T_c with a jump width less than 0.2 K and a hysteresis loop width of 10 K, and 2) resistivity increased linearly with temperature in metallic phase.[15]

For X-ray diffraction studies, we used a Bruker diffractometer[16] operated in the "scissors mode" in which the powder sample remains fixed and both the X-ray source and detector move symmetrically to vary the Bragg angle. Under such conditions the powder in a specimen cannot move during a scan. A graphite monochromator was used to remove the copper K_β line from the XRD, but the copper $K_{\alpha 1,2}$ doublet is unresolved. Single crystal alignment and characterization was carried out with the aid of a Gas Area Detector Diffractometer (GADD).

V *K*-edge XANES data were obtained at the X–11A beam line at the National Synchrotron Light Source (NSLS). The beamline uses a double crystal Si (111) monochromator

providing energy resolution of $\Delta E/E = 10^{-4}$. The monochromator crystals were detuned 40% to reduce harmonics. For the single crystal XANES on pure V_2O_3, thin (15 μm) crystals had the hexagonal a-c plane parallel to the sample surface and were measured in transmission mode at room temperature (PM) and 60 K (AFI). For single crystal samples containing Cr, XANES data were obtained using the glancing emergent angle (GEA) method, reported independently by Pease *et al.*[17] and by Suzuki,[18] to minimize the fluorescence distortion effect. Samples were aligned to have a (110) flat using GADD in order to obtain XANES for parallel and perpendicular orientations of X-ray polarization vector relative to the crystal *c* axis. For the single crystal sample with x = 0.004, however, the main edge V *K* edge XANES was anomalously broadened, in a manner that suggests the possibility of more than one c axis direction. We do not publish or further analyze the single crystal data from the x = 0.004 sample here. Powder samples for transmission studies, measured at room temperature, were prepared by grinding and rubbing onto tapes by standard methods. For temperature dependent measurements, powders were ground and mixed with BN binder, then compressed into flat pellets. The samples were then heated in a furnace having a Kapton window, under flowing nitrogen.

The GEA method is used to reduce the over-absorption effect that arises in XANES studies of concentrated bulk samples measured by the fluorescence method. Some details of the GEA method need to be briefly reviewed. In the GEA mode, we used normal incidence to the crystal flat and, by blocking the beam to the ion chamber, restricted the detected fluorescence to a small angle, which in our case was of the order 3° Since only a small solid angle of radiation can be used in GEA, GEA data from single crystals have enhanced noise to signal ratio, relative to transmission powder results. In principle, the GEA method can never completely remove the fluorescence distortion. This assertion is evident in Ref. 17, in which it was shown that no matter how small the GEA angle, the fluorescence observed XANES from bulk copper always has a small, residual distortion relative to that observed using a copper foil in transmission. Recently, Frenkel *et al.*[19] compared single crystal XANES obtained from single crystals of 2.9% Cr doped $(Cr_xV_{1-x})_2O_3$ with transmission powder XANES from the same material. To make this comparison, a composite single crystal spectrum of 2/3 the E perpendicular c axis spectrum with 1/3 the E parallel to the c axis spectrum was compared to the powder transmission XAFS.[19] The agreement was excellent. However, an unexplained aspect of this experiment was that the fine

structure peaks were somewhat better resolved and stronger in the GEA than for the powder transmission data. This observation is opposite what is expected and is opposite to that observed for copper metal in reference sixteen. This finding implies that for the $(Cr_xV_{1-x})_2O_3$ system, some small unexplained distortion of the XANES is taking place associated with the manufacture of the powder sample itself.

Our computations were performed by the full multiple scattering method within Green's function formalism by a spin-polarized version of XKDQ code.[20] Both dipole and quadrupole parts of electron-photon interaction were taken into account. Spectra were calculated using 51-atom clusters and it was checked that the increase of cluster size up to 137 atoms does not change any features of XANES and pre-edge structure. The electron configurations of the absorbing atoms ($1s^1 3d^{2.9}$) included the 1*s* hole and additional 0.9 electrons at 3*d* level as a screening charge. The exchange correlation potential was taken in the Xα approach. To simulate a finite life time of electron-core excitation and experimental resolution, calculations were performed at complex energy. Since the length of the photoelectron mean free path is not known for the low-energy region, the broadening of the spectra was calculated by employing a semi-empirical energy dependence of the width of the electron-hole excited state. The resultant spectra are the averages of two calculations with the spin of the photoelectron being parallel and anti-parallel to the spin of the absorbing atom. Calculations were carried out for pure V_2O_3, both in the PM and AFI structures, for both E||*c* and E⊥*c* orientations of the XANES.

III. RESULTS

A. X-ray diffraction

Two kinds of XRD powder diffraction scans were obtained. We obtained full range scans that covered many peaks. Within the scatter of the data these scans were in agreement with the standard V_2O_3 pattern for the corundum structure, except that for samples with mixed conducting and insulating phase some peaks were split. We also obtained data with short angular range but better counting statistics in the vicinity of the (110) reflection (hexagonal indexing). All XRD data were obtained at room temperature (Fig. 1). The XRD corresponding to Fig. 1 were obtained less than a week after grinding single crystals to a powder. The pure V_2O_3 powder data

was obtained from freshly ground single crystals of pure V_2O_3 prepared at Purdue. All samples of this group correspond either to a single corundum phase $x = 0$ (PM), 0.029 (PI), and 0.052 (PI) or contain both metallic and insulating phases ($x = 0.004$, 0.012). We limit our discussion here to the scans in the vicinity of the strong (110) peak, obtained with better counting statistics. The (110) XRD of single-phase samples agree closely with results of McWhan and Remeika.[1] As expected, we observe a shift in the *a* lattice parameter between PM and PI phases. We obtain a value for the *a* parameter of 5.2 % Cr in V_2O_3 that agrees within less than 0.01 Å of the McWhan–Remeika value of 5.00 Å. Our *a* value for pure V_2O_3 is about 0.016 Å less than the McWhan–Remeika value of 4.95 Å. The powder camera values for the *a* parameter as obtained by McWhan and Remeika[1] are to be preferred to ours, and are obtained by a better technique for this particular purpose than use of our modern laboratory diffractometer.[21] In any case, these differences in absolute value of the *a* parameter are not significant in the present context.

We noticed puzzling features in our XRD results for several compositions, as shown in Fig. 1:

A) $x = 0.004$. On the phase diagram reported by Kuwamoto *et al.*,[10] a diagram that shows a region of thermal hysteresis between insulating and conducting phases, this composition is outside the two-phase region at room temperature. In our data a strong insulating phase $K_{\alpha 1,2}$ doublet exists for the sample. From a measurement of the relative intensities between M phase and I phase peaks shown for this composition in Fig. 1, the concentration of the insulating phase in the sample is about 26%. We speculate that the pronounced insulating phase fraction for a composition that is expected to be pure conducting phase at room temperature may have to do with a rapid quench resulting from the skull melting procedure

B) $x = 0.012$. The concentration of PM in this sample appears to be about 17% which is significantly less than the value of 30% reported by McWhan and Remeika for this composition.[1] For the $x = 0.012$ concentration, the metallic phase peaks are significantly shifted to the lower angle side relative to pure V_2O_3.

C) $x = 0.029$. This sample has an anomalous shape of the XRD $K_{\alpha 1,2}$ line. The composition should be single phase insulator according to the phase diagram.[10]

We obtained XRD from a second specimen with $x = 0.004$ to compare with the XRD of our first $x = 0.004$ specimen as shown in Fig. 1. Again, coexisting M and I phases were observed. However, the concentration ratio between the two phases was different between the $x = 0.004$ sample referred to in Fig. 1 and the second sample of the same $x = 0.004$ composition. We found variations in the ratio of the two phases between different samples of the $x = 0.012$ ingot as well. From early results of McWhan and Remeika,[1] these results are not surprising. For samples with coexisting conducting (M) and insulating (I) phases the ratio of I to M phase was found by McWhan and Remeika[1] to vary substantially with past thermal history, and it is quite conceivable that thermal history may vary from place to place within an ingot of these materials as made by skull melting.

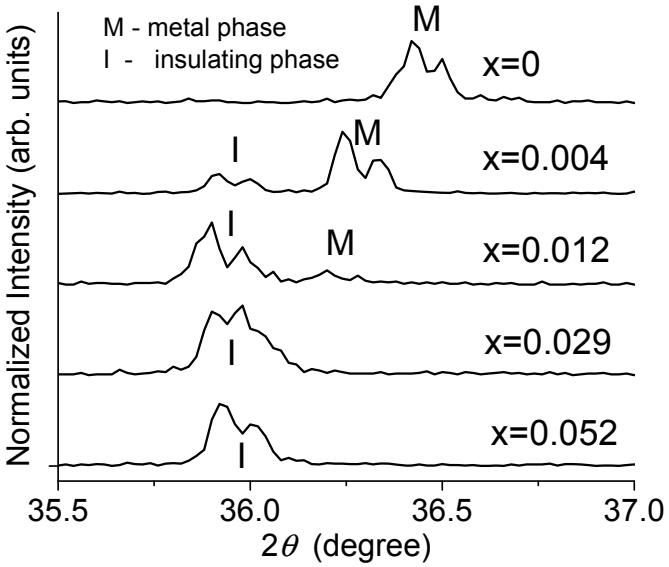

Figure 1. XRD patterns of (110) reflection for powders ground from bulk crystals of $(Cr_xV_{1-x})_2O_3$ for various concentrations. All samples were measured within one week after grinding their respective single crystals. These XRD peaks all show the unresolved $K\alpha_{1,2}$ doublet, but the shape of the doublet is anomalous for the $x = 0.029$ sample. The curves are shifted vertically for clarity.

Finally, we found that one sample of 1.2% Cr in V_2O_3, when studied by a powder XRD experiment that commenced within a few minutes of grinding the crystal into a powder, changed its (110) XRD pattern slowly with time in an overnight scan. The intensity of the metallic phase

$K\alpha_{1,2}$ doublet, relative to the insulating phase $K\alpha_{1,2}$ doublet, was initially large but decreased with time after grinding. An unexpected new XRD feature observed only in the insulating phase $K\alpha_{1,2}$ doublet of this same powder sample also decreased with time after grinding. These were surprising observations; and although we have documented our results, we are not presently ready to present publishable data on the effect, since our overnight XRD spectrum on this sample comprises a time average of results. To study the effect rigorously a synchrotron based XRD experiment is required.

One conclusion we draw from these various XRD observations is that for samples in the coexistence (two phase) concentration regime, the ratio of metallic to insulating phase can vary within a sample batch of uniform concentration of Cr, if the samples are made by skull melting.[14] As pointed out above, McWhan and Remeika[1] long ago found that the ratio of metallic to insulating phase for compositions within the two phase region varies quite sensitively with thermal history of the sample. Samples of similar two phase composition made by just this same skull melting method have been used in many experiments by others, and thus our finding of a variation of metallic to insulating phase ratio for two phase samples made by skull melting is therefore of interest in itself.

B. X-ray absorption near edge structure

The energy scans of the absorption coefficients in the *K*-edge region for selected samples can be found in Ref. 19 and Fig. 6 below. Figures 2(a) and (b) focus on the V *K* pre-edge regions of the following single crystal samples: AFI phase pure V_2O_3, PM phase pure V_2O_3, $(V_{1-x}Cr_x)_2O_3$ x = 0.012, 0.029, and 0.052 with both polarization directions included in the data. In agreement with Rodolakis *et al.*[6] the pre-edge region features the peaks A and B are followed by the structure C for the x = 0.012 sample. These details become more prominent after subtracting the base line.

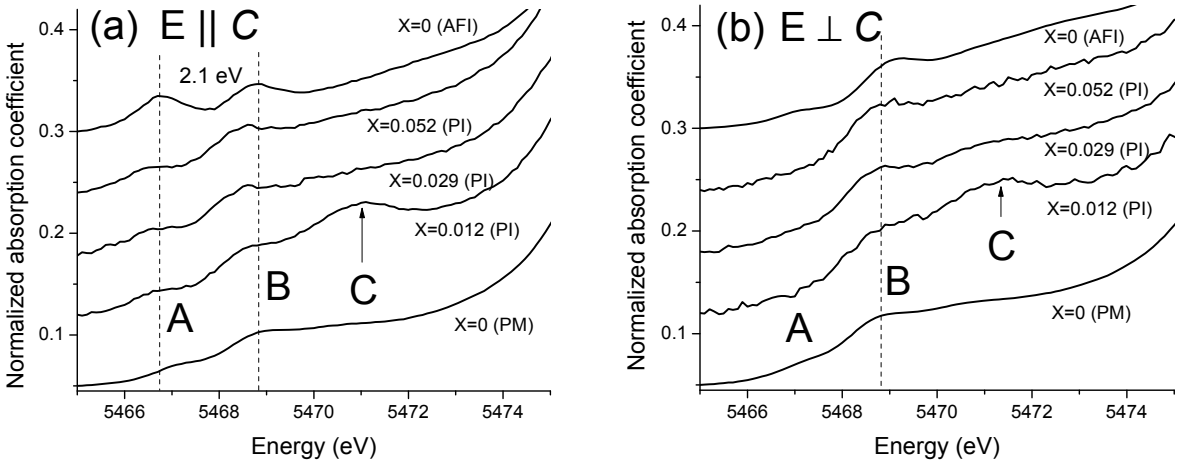

Figure 2. Polarization-dependent V K-edge XANES obtained for single crystals of $(Cr_xV_{1-x})_2O_3$. (a) Polarization vector is parallel to the hexagonal *C*-axis, (b) perpendicular. The curves are shifted vertically for clarity.

All XANES figures below show absorption coefficient data normalized by the edge step. Peaks A and B vary more or less systematically with Cr concentration. This is not the case for the C structure. This structure has the maximum intensity for $x = 0.012$ (indicated by arrows) and is also weakly observable at $x = 0.029$ in $E \perp c$ orientation. It is quite evident that this feature in the spectrum for $x = 0.012$, which is a mixture of M and I phases, cannot be represented as a linear combination of pure PM and pure PI XANES.

We then compare the XANES of three single crystals obtained by the GEA method, with transmission XANES for powder samples of the same compositions at room temperature. In crystals with trigonal symmetry, such as PM phase of V_2O_3, simulated powder data can be compared to the weighted average of spectra of the two perpendicular orientations of *c* axis (relative to the *E* vector). The (1/3 [$E||c$] + 2/3 [$E \perp c$]) spectra of single crystals and spectra of powder samples are superimposed in Fig. 3. This method is only an approximation, even for the perfect crystals, since it assumes that XAS is dominated by dipole contribution only. We note, however, that the pre-edge features are caused also by quadrupole contributions, and their angular dependence should be different from the one dictated by the dipole contribution only. This complication may contribute to slight discrepancies between single crystal and powder data for the peaks A and B region in Fig. 3. These discrepancies are much smaller than the

pronounced enhancement of peak C for the two phase samples which are the subject of this study. This issue is discussed further in Section IV.

It may be seen that pre-edge structure features are nearly consistent between single crystal and powder data, except for the region of peak C for the two phase sample $x = 0.012$ and the region of peak C for the sample with $x = 0.029$. The data are also completely consistent in the region of the main edge. We note that in the powder data of Rodolakis, *et al.*[6] for their $x = 0.011$ sample, the C region is different than we observe for our $x = 0.012$ powder data. In the former work done with the $x = 0.011$ powder sample peak C is somewhat enhanced relative to that we observe for our $x = 0.012$ sample. This enhancement might be caused by a different thermal history during skull melting of our sample relative to that of the sample of Rodolakis, *et al.*[6]

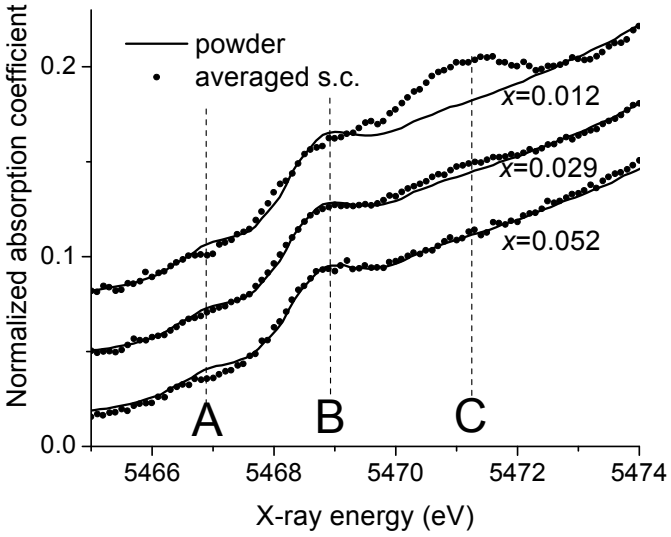

Figure 3. Comparison of the orientationally averaged V *K* pre-edge data obtained for the $(Cr_xV_{1-x})_2O_3$ single crystals and the powder samples obtained by grinding single crystals of the same composition. Note the dramatic enhancement of the feature C in the single crystal relative to the powder for the composition corresponding to the mixed phase ($x = 0.012$). Much smaller enhancement is also noticeable for the $x = 0.029$ sample. The curves are shifted vertically for clarity.

Finally, we studied the temperature dependences XANES of the $x = 0$, 0.004 and 0.052 powder samples (Fig. 4 below). For all temperatures studied, a pure V_2O_3 sample remains in PM phase whereas the $x = 0.052$ sample remains in PI phase. For both these single phase samples the

amplitudes of the peaks B and C monotonically increase with the temperature. For $x = 0.004$, the phase diagram of Kuwamoto *et al.*[10] indicates that the composition is just at the border of a two phase region of the phase diagram, which exists between T ~ 350 K and 450 K. Such a high temperature two-phase region was experimentally observed by Jayaraman *et al.*[8] for a sample with $x = 0.006$. The most prominent feature of the temperature dependence of this spectrum is that the intensity of the structure C abruptly increases when the temperature changes from ambient to 400 K. The 400 K temperature is the only temperature investigated in this study that belongs to the two-phase region of the diagram. When the temperature raises from 400 K to 500 K the intensity of the structure C slightly decreases but still is considerably greater than for other three temperatures. After the increase of the temperature up to 623 K structure C returns to a magnitude typical for one-phase sample. These results are shown in Fig. 4.

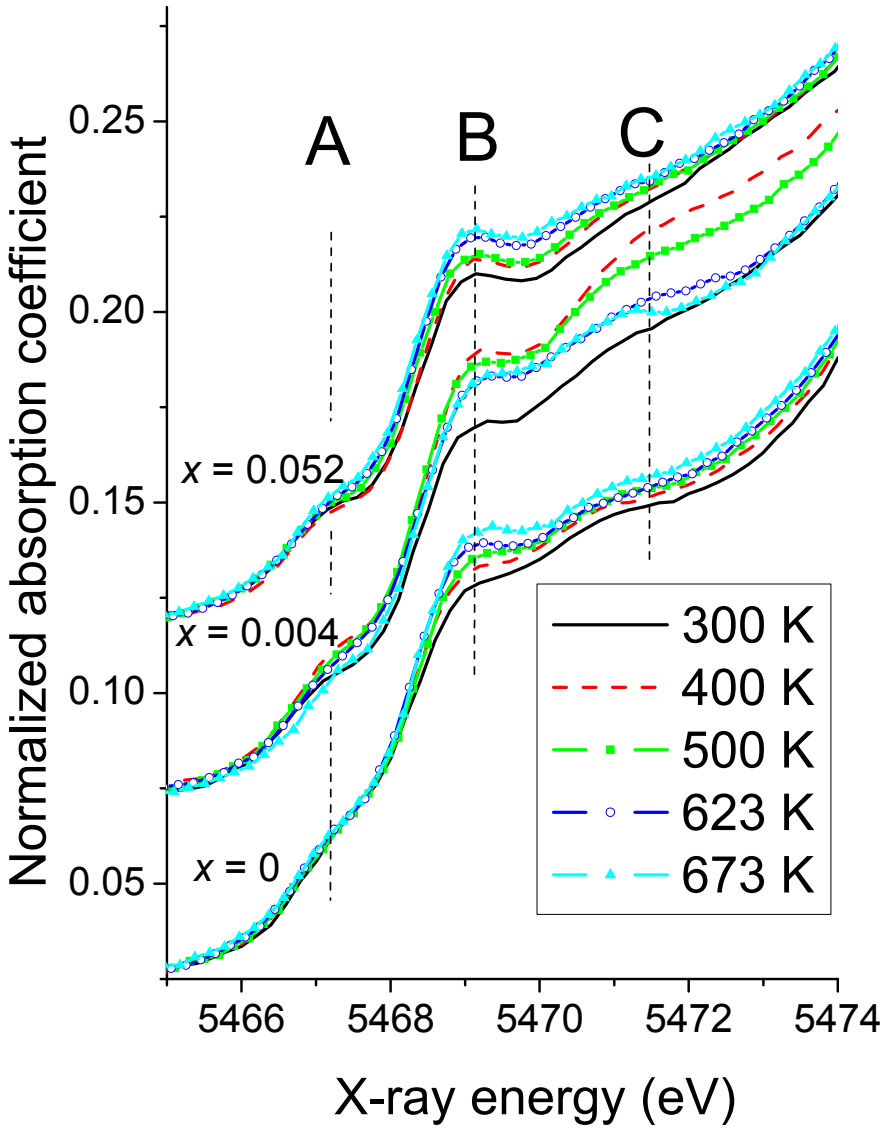

Figure 4. Temperature dependence of V K-edge XANES data obtained for the $(Cr_xV_{1-x})_2O_3$ powders. The features A,B,C change monotonically with temperature for single phase (x = 0 and x = 0.052) concentrations. Note the non-monotonic behavior of the peak C for the mixed phase region in the x = 0.004 sample. The curves are shifted vertically for clarity.

C. Photoemission

Our investigation into the XRD of different sections of single crystals of the same composition, in the coexistence regime, was motivated by an interesting situation that has arisen in regards to recent photoemission studies carried out by others.[5] These studies are now briefly discussed. We

noticed that one of the samples investigated by Mo *et al.*[5] was 1.2% Cr doped V_2O_3 at room temperature. For this composition, using their sample synthesis methods, McWhan and Remeika[1] report fully 30 % conducting phase in a predominantly insulating matrix. Since recent studies show that metallic phases in the Cr doped V_2O_3 system show a quasi particle peak spectral shape in photoemission, and insulating phases do not, then in one simple interpretation of previous evidence there could be a mixture of 30% quasi particle peak spectrum and 70% insulator spectrum in the photoemission of material with 1.2% Cr at room temperature. We simulated such a spectrum assuming 20% metallic and 80% insulating phase, as shown in Fig 5 (narrow line). No such experimental spectrum has been observed. This finding lead us to explore how much variation there might actually be between conducting and insulating phase ratios within a sample batch of uniform Cr concentration. We found that for samples of the same composition of x = 0.012, there can be markedly differing ratios of M to I phases within different regions of the same ingot as made by skull melting. It would be of interest to investigate such a photoemission spectrum on a single crystal specimen that is known to have a substantial fraction of metallic phase mixed into the predominantly insulating phase.

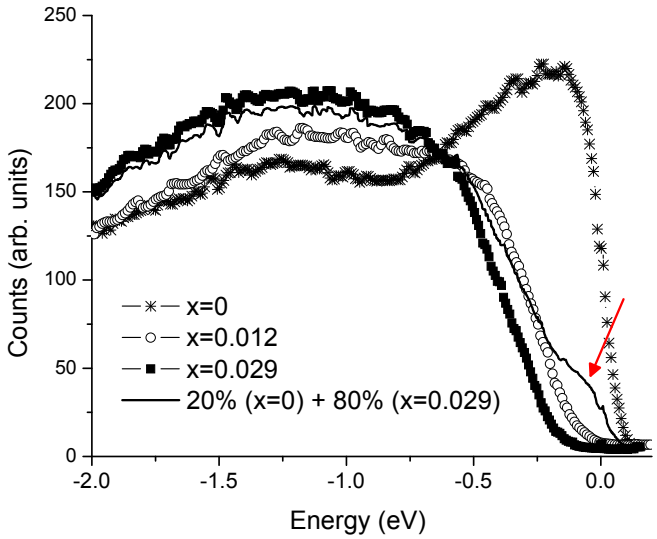

Figure 5. Simulated spectrum from photoemission (Ref. 5) for 80% fully I phase (2.9% Cr), and 20% fully M phase (pure PM phase V_2O_3). The simulated spectrum is the dotted line and shows a strong high energy feature, shown by arrow, not seen in the experimental curve for two phase room temperature material with x = 0.012.

IV. DISCUSSION

An interesting interpretation of the pre-edge structure in V *K* XANES was given by Rodolakis *et al.*[6] by studying powdered samples.[6] In the present paper, we report on the comparison of the single crystal and powder measurements, that allowed us to take another look at the origin of the pre-edge structure by contrasting these two types of samples.

First, let us describe the lowest vacant electronic states of V_2O_3 corundum crystal, which determine the structure of the pre-edge region, within a simple one-electron approach neglecting electron correlation. Antibonding hybridized V 3*d*-O 2*p* orbitals in an ideal [VO_6] octahedron split into lower t_{2g} orbitals and upper e_g. A trigonal "umbrella" distortion of those octahedra in V_2O_3 corundum lattice breaks inversion symmetry transforming the e_g representation to e^{σ} and further splits the t_{2g} representation into a and e^{π}. The superscripts σ and π at e representation just denote the type of hybridization of corresponding atomic orbitals. It is worth noting that the hybridization of V 3*d* with O 2*p* orbitals for e^{σ} representation is more intensive than for the e^{π} case.

Information from the literature about the values of the $t_{2g} - e_g$ and following $a - e^{\pi}$ splittings seems somewhat controversial. In the framework of semi-empirical crystal field split approach, Rodolakis *et al.*[6] used 2 eV and 0.3 eV, whereas Park *et al.*[22] used 1eV and 0.05 eV respectively. Our FMS calculations result in 1.8 eV and 0.01 eV. Despite these discrepancies, one can state that trigonal splitting of the t_{2g} states is negligible in comparison with the width of even the lowest-energy pre-edge peak A.

According to the final state rule,[23] the Hamiltonian employed for the calculations of the XANES includes the potential of the properly screened core hole. This attractive potential shifts localized V 3*d* states down by about 2 eV. As a result, in the paramagnetic insulators, antibonding t_{2g} and sometimes e_g states of an absorbing TM atom appear to be well below the bottom of the conduction band. That is why the pre-edge peaks corresponding to the excitation of the core electron to these states are often called X-ray excitons.

There is a consensus now that the electron configuration of the ground state of the vanadium ion in V_2O_3 is a triplet formed by superposition of the ($e^{\pi}\uparrow$, $e^{\pi}\uparrow$) and ($a\uparrow$, $e^{\pi}\uparrow$) two-electron states.[22,6] Therefore, as it was pointed out by Rodolakis *et al.*,[6] the lowest energy pre-

edge peak A corresponds to an X-ray exciton with three t_{2g}-electrons in high-spin configuration ($a\uparrow$, $e^{\pi}\uparrow$, $e^{\pi}\uparrow$) or ($e^{\pi}\uparrow$, $e^{\pi}\uparrow$, $e^{\pi}\uparrow$).

The value of t_{2g}-e_g crystal field splitting just corresponds to the energy separation between peaks A and B. Therefore excitation of 1*s* electron to $e^{\sigma}\uparrow$ contributes to the peak B. The magnitude of the exchange interaction for V^{+3} is also about 2 eV. The transitions to $t_{2g}\downarrow$ hence are the second part of the contribution to the peak B whereas transitions to $e^{\sigma}\downarrow$ contributes to a broad structure C. At first glance it is strange that the structure C is so weak at room temperature for most samples. In many octahedrally coordinated TM oxides with metal ions in both $3d^0$ and paramagnetic states there are peaks in the pre-edge structure caused by excitation of photoelectrons to 3*d* states of neighboring metal atoms. There could be two reasons which suppress displaying these transitions as a pronounced peak. 1) There are too many different final states which make this structure quite broad. 2) The low-energy photoelectron free path is too short in V_2O_3 which also smears the structure. (The origin of the C structure in the spectra of the x = 0.012 single crystal sample and the x = 0.004 powder sample at 400 K will be discussed separately.)

The interpretation of pre-edge structure given above is confirmed by calculations presented in Figs. 6 and 7. The energy scale, unique for all calculated spectra, was aligned with that for experimental data to achieve the best agreement in the range of the main edges. The agreement between calculated and experimental spectra in the main edge region (Fig. 6) is excellent for both polarization directions. Calculations of the pre-edge yield quite reasonable energies and amplitudes for peaks A and B (Fig. 7). One can see that the peak A in some calculated spectra is more intense than in the experimental ones. We point out two further issues that affect comparison between theory and experiment:

First: the quadrupole contributions to pre-edge peaks can cause the intensities of these features to be dependent on the direction of the x-ray *k* vector for single crystal XANES. The theoretical calculation of this angular dependence requires experiment input not available to us. Brouder has shown[24] that accurately angular resolved data must be obtained for several different *k* vector directions in order to analyze the quadrupole contribution. Our experimental studies were carried out for the purpose of obtaining not only XANES but also EXAFS so that the great majority of data collection was by necessity on regions of the x ray absorption spectra that are

described accurately by the dipole approximation alone. We have, however, calculated the maximum angular variation due to the quadrupole contribution and found that these variations are considerably less intense that the pronounced C structure enhancement observed in the two phase state that is the main topic of this study.

Second: the one-electron multiple scattering approach calculates the transition rate to both vacant and occupied electron states; hence our calculations correspond to transitions to completely empty t_{2g} states, whereas two of these states are occupied.

In principle, the angular dependence of the pre-edge peak A gives a new opportunity to determine experimentally the electron configuration of the ground state. The ground state configuration determines the weights with which 1*s* electron excitations to *a* and e^{π} final states contribute to the peak A intensity. Since the probabilities of $1s \rightarrow a$ and $1s \rightarrow e^{\pi}$ transitions are different and can be calculated theoretically for a given atomic configuration for every polarization and wave vector directions, the measured angular dependence enables one to determine the weights. As was mentioned earlier, both dipole and quadrupole parts of the electron-photon interaction contribute to the peak A intensity. In slightly distorted $[TMO_6]$ octahedra the quadrupole part practically does not depend on the octahedron distortion. In contrast, the dipole contributions caused by the *p*-*d* mixture due to breaking the central symmetry strongly depend on instantaneous local atomic structure. The determination of the ground state is beyond the scope of the present article.

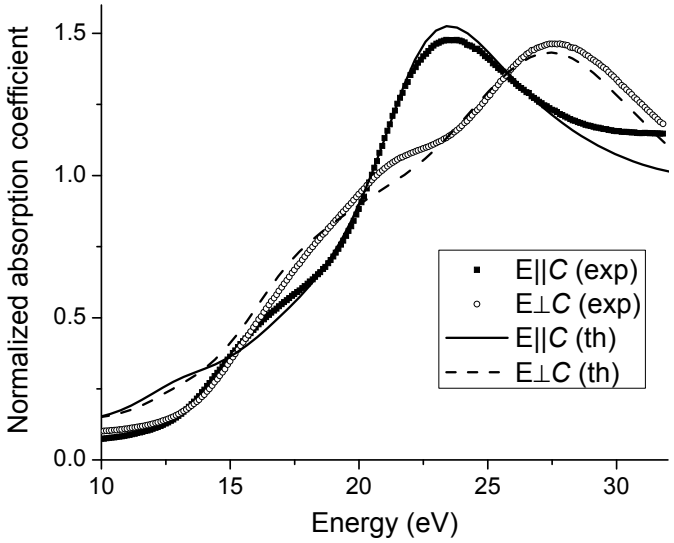

Figure 6. Comparison of experimental and calculated spectra for the main edge region in V_2O_3 single crystals for two different orientations of X-ray polarization vector. The data were taken in fluorescence at room temperature.

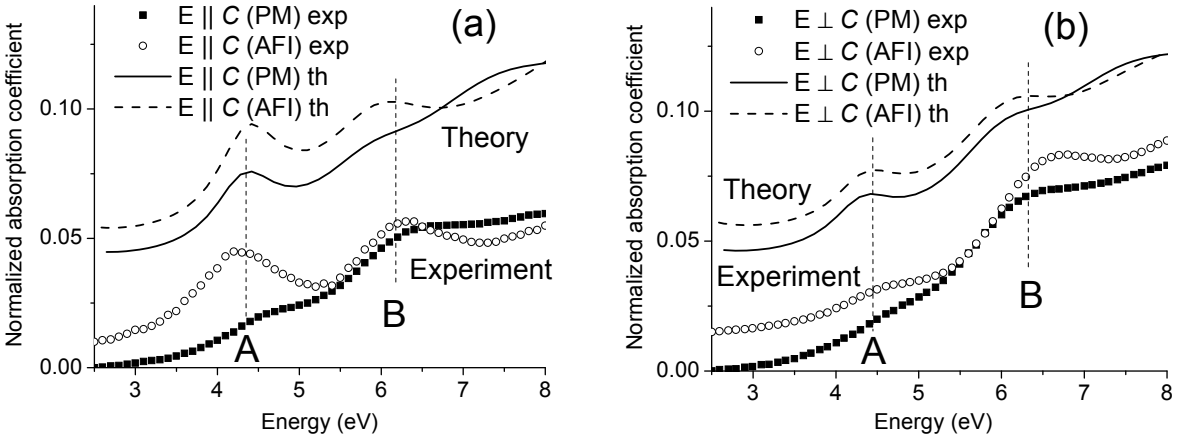

Figure 7. Pre-edge regions in the polarization-dependent V K-edge in V_2O_3. Shown are the data (symbols) and theory (lines) for the AFI and PM phases. The curves are shifted vertically for clarity.

Another confirmation of our interpretation of the pre-edge peaks is given by the temperature dependence of pre-edges for pure V_2O_3 and $x = 0.052$ powder samples as shown in

Fig. 4. Both samples exhibit a monotonic increase of B and C intensities with the temperature increase and do not change outside these regions. Since both samples remain in the single phase states through the whole temperature interval studied, the only change of the atomic structure, except the weak increase of lattice constants, is the growing of the amplitude of temperature vibrations which in turn results in the increase of the mean squared displacement of the V atom from the instantaneous center of an oxygen octahedron. It was shown both experimentally and theoretically that such an increase results in an enhancement of the pre-edge peaks that are caused by photoelectron excitation to e_g states. This effect has previously been observed in a number of crystals with octahedrally coordinated paramagnetic TM ions $EuTiO_3$ and $SrTiO_3$.[25,26] Since in V_2O_3 transitions to e^{σ} states contribute to the both B and C peaks, both of them enhance with the temperature increase. We illustrate our conclusion by simple simulation of the effects of thermal vibration. We calculated the V pre-edge in the same 51-atom cluster but with absorbing V ions being displaced, in turn, toward each of neighboring O atoms by 0.06 Å. The average of these calculations is shown in Fig. 8.

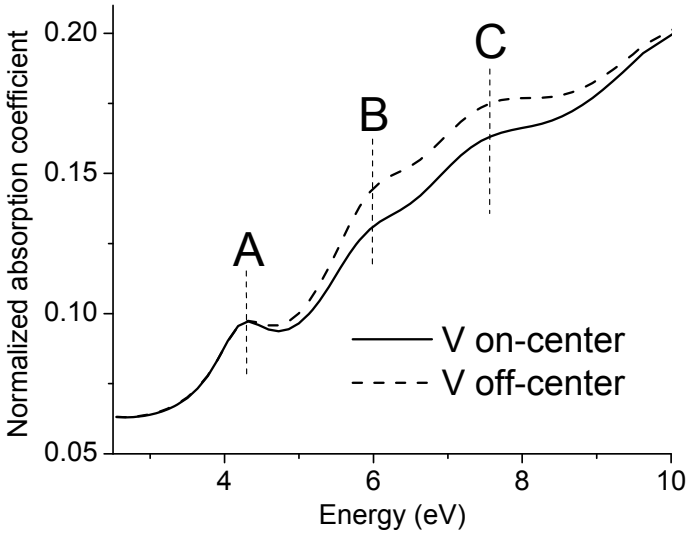

Figure 8. Theoretical calculations of angular-averaged, pre-edge features carried for undistorted (solid) and distorted (dash) configurations of local V environment in V_2O_3. Distortions were introduced by displacing V atoms in the simulated cluster toward nearest O atoms.

In conclusion, we will offer a speculative model for the appearance of the peak C in the spectra of $x = 0.012$ single crystal and the "anomalous" temperature dependence of the same region for $x = 0.004$ single crystal. First, note that according to Kuwamoto *et al.*[10] $x = 0.012$ is the only two-phase sample at room temperature among those studied, whereas, the $x = 0.004$ powder sample crosses the two-phase region during heating. Second, the vanadium *K* pre-edge structure in V_2O_5 crystal, $VOPO_4$ xerogel, and other compounds with vanadium ions in highly distorted oxygen octahedral environments contain an intense peak with magnitude close to the main edge step.[27–30] The energy of this peak coincides with that of the C peak in the $x = 0.012$ sample spectrum but the area under the peak in V_2O_5 exceeds that in $x = 0.012$ sample by about 100 times. A possible explanation of the peak C origin in $x = 0.012$ single crystal is that after two-phase crystal quenching about 1% of V atoms placed on the phase boundaries appear in distorted environments, due to the different structures of the coexisting PI and PM regions, and produce corresponding contributions to the C peak. This distorted part of the crystal structure creates strain which releases when the crystal is ground during powder sample preparation; regular oxygen octahedra restore, and therefore the C peak may diminish in an $x = 0.012$ powder sample spectrum relative to the single crystal. We point out that Rodolakis *et al.*[6] observe an enhanced intensity of peak C region for a powder sample with $x = 0.012$, but this peak C disappears when the sample is lowered in temperature so that it is single phase. However, the intensity of peak C in the room temperature powder sample with $x = 0.012$ observed by Rodolakis *et al.*[6] is much less than what we observe for our single crystal sample of the same composition. Furthermore, when our $x = 0.004$ powder sample is heated and crosses the two-phase region a small fraction of V ions also appears in a highly distorted environment which, again, results in a distortion of the C structure in the pre-edge. When the temperature exceeds 600 K and the sample again falls into the one-phase region the usual pre-edge structure restores, but with enhanced magnitudes of the B and C peaks as in the cases of $x = 0$ and 0.052 powder samples.

Our analysis, cumulatively, indicates existence of distorted structures in a mixed phase single crystal. We also found that in one case, when the XRD was observed within minutes of grinding the single crystal to a powder, the XRD pattern changed with time overnight. A possible explanation is that there can be metastable phases related to the coexistence of two types of

environments, and the grinding relieves internal stresses. Furthermore, if there is a mixture of M and I phases, since the pure M and pure I phases have quite different c/a ratios then the interfacial region between the two different crystal structures would be expected to be disordered, and it is possible that distorted VO_6 octahedra could result along the interfacial surfaces. Wong *et al.*[30] carried out a careful study of the XANES for several oxides of V, but their graphical data is not published on a large enough scale to view the pre edge structures well. On the other hand, Vining *et al.*[31] have made a direct comparison of the XANES of V_2O_5 and PM V_2O_3. From this comparison it may be seen that the peak C observed by both us and Rodolakis *et al.*[6] in a composition with $x = 0.011$ or $x = 0.012$ (present study), is located rather close in energy to the position of the major XANES peak observed by Vining *et al.*[31] for V_2O_5. The V_2O_5 structure contains a markedly distorted VO_6 octahedron that results in a pronounced XANES peak that is just at the energy of our large peak in single crystal, 1.2% Cr doped V_2O_3, supporting our suggestion that it is such distorted octahedra at the interface between two different crystal structures in the two phase samples that give rise to the enhanced peak C. It is further of interest to note that experimentally as one decreases the Cr composition from the pure I regime at room temperature toward the mixed I and M phase regime ($x = 0.029$), a precursor of peak C is observed, but only for the electric vector perpendicular to c axis orientation.

V. SUMMARY AND CONCLUSIONS

We have obtained V *K* edge XANES for a series of single crystal specimens of $(Cr_xV_{1-x})_2O_3$, for various Cr concentrations. For Cr concentrations corresponding to single phase material according to the phase diagram of Kuwamoto *et al.*,[10] two pre edge features we call peak A and peak B vary systematically with concentration and show a dependence on orientation of the photon electric vector direction that agrees approximately with theory. On the other hand, there is a pronounced peak C for both polarization directions in the XANES of a sample with $x = 0.012$, which is expected to be in the two phase "coexistence" regime at room temperature. This peak occurs at about 5471 eV. We observe a much weaker enhancement of the XANES in this energy region for a sample with $x = 0.029$, for one orientation only of the electric vector. We point out for the first time that peak C is associated with the two phase, or coexistence regime of the $(Cr_xV_{1-x})_2O_3$ system, which is characterized by coexisting metal and insulating phases with

different crystal structures. Thus, the feature diminishes or disappears for Cr concentrations corresponding to the single phase regions of the phase diagram. We find that if we raise the temperature of a powder specimen of $x = 0.004$ material, systematically from room temperature to 630 K, for intermediary temperatures near the two phase region of the phase diagram, a peak near 5471 eV develops, then the peak diminishes when the temperature is again in a single phase region.

We propose a model for "peak C." We point out that the energy position of this feature is close to that expected for the V K edge XANES of V atoms in strongly distorted VO_6 polyhedra, such as are found in V_2O_5 or xerogel.[27,30] This feature is found to be so pronounced in these materials, that only ~ 1% of V atoms in such polyhedral would markedly effect the V K edge XANES. We suggest that in the coexistence regime, the interface between insulating and metallic phases will be markedly strained, and that this strain is associated with peak C.

As part of our sample characterization, we have also determined that for samples in the two phase, or coexistence concentration region as made by skull melting, the ratio of metal to insulating phase concentration varies markedly from region to region for material with uniform Cr concentration. This finding is completely to be expected based on old studies by McWhan and Remeika,[1] if indeed different portions of an ingot of $(Cr_xV_{1-x})_2O_3$ as made by skull melting cool down with different thermal histories. For one sample with $x = 0.012$, we observed that a powder specimen observed within a few minutes of grinding from a single crystal exhibited an XRD pattern that changed systematically overnight. Other investigators have used samples of nearly the same composition, made by the same skull melting method, and therefore, these complications of the XRD interpretation apply to other experiments besides those reported here. In particular, if a room temperature PI sample with $x = 0.012$ were to have the 30% concentration of metallic phase as was reported for one of the specimens studied by McWhan and Remeika,[1] in a simple model one would expect a noticeable quasi particle peak in photoemission, where we point out that in fact, so far none is observed (Fig. 5).

Finally, we point out that the two phase region of this system is not only of fundamental interest, as pointed out by the theory of Park *et al.*[9] The ratio between the metallic and insulating phases in the coexistence region can depend on thermal history, and we find evidence that interfacial strains between the coexisting phases in the coexistence region of the phase diagram

can have pronounced effects. Since any device that uses the $(Cr_xV_{1-x})_2O_3$ system as a switch of some sort by changing between PI and PM states would be influenced by changes in the ratio of phases and consequent changes in interfacial strains as one traverses the coexistance region, our findings may have device implications.

Acknowledgements

The authors acknowledge support by the U.S. Department of Energy Grant No. DE-FG05ER36184.The NSLS is supported by the Divisions of Materials and Chemical Sciences of Department of Energy. PNC/XOR is supported by the U. S. Department of Energy, NSERC of Canada, University Washington, Simon Fraser University, Pacific Northwest National Laboratory, and the Advanced Photon Source is supported by the U. S. Department of Energy under Contract No. W-31-109-Eng-38.

References

1 D. B. McWhan and J. B. Remeika, Phys. Rev. B2, 3734 (1970).

2 L. F. Mattheiss, J. Phys. Condens. Matter 6, 6477 (1970).

3 K. Held, G. Keller, V. Eyert, D. Vollhart, and V. I. Anisimov, Phys. Rev. Lett. 86, 5345 (2001).

4 S. K. Mo, J. D. Denlinger, H. D. Kim, J. H. Park, J. W. Allen, A. Sekiyama, A. Yamasaki, K. Kadono, S. Suga, Y. Saitoh, T. Muro, P. Metcalf, G. Keller, K. Held, V. Eyert, V. I. Anisimov, and D. Vollhardt, Phys. Rev. Lett. 90, 186403-1 (2003).

5 S. K. Mo, H. D. Kim, D. D. Denlinger, J. W. Allen, J. H. Park, A. Sekiyama, A. Yamasaki, S. Suga, Y. Saitoh, T. Muro, and P. Metcalf, Phys. Rev. B74, 165101 (2006).

6 F. Rodolakis, P. Hansmann, J. P. Rueff, A. Toschi, M.W. Haverkort, G. Sangiovanni, A. Tanaka, T. Saha-Dasgupta, O. K. Anderson, K. Held, M. Sikora, I. Alliot, J. P. Itie, F. Baudelet, P. Wzietek, P. Metcalf, and M. Marsi, Phys. Rev. Lett. 104, 047401 (2010).

7 C. Gougoussis, M. Calandra, A. Seitsonen, C. Brouder, A. Shukla, and F. Mauri, Phys. Rev. B 79, 045118 (2009).

8 A. Jayaraman, D. B. McWhan, J. P. Remeika, and P. D. Dernier, Phys. Rev. B 2, 3751 (1970).

9 H. Park, K. Haule, and G. Kotliar, Phys. Rev. Lett. 101, 186403 (2008).

[10] H. Kuwamoto, J. M. Honig, and J. Appel, Phys. Rev. B 22, 2626 (1980).

[11] C. Meneghini, S. D. Matteo, C. Monesi, T. Neisius, L. Paolasini, S. Mobilio, C. R. Natoli, P. A. Metcalf, and J. M. Honig, Phys. Rev. B 72, 033111 (2006).

[12] Y. Joly, S. D. Matteo, and C. R. Natoli, Phys. Rev. B 69, 224401 (2004).

[13] M. Cuozzo, Y. Joly, E. K. Hlil, and C. R. Natoli, in *Theory and Computation for Synchrotron Radiation Spectroscopy*, edited by M. Benfatto, C. R. Natoli, and E. Pace (AIP, Melville, NY, 2000), 45.

[14] P. Metcalf and J. Honig, *Current Topics in Crystal Growth Research* 2, 445 (1995).

[15] A. I. Frenkel, E. A. Stern, and F. A. Chudnovsky, *Solid State Commun*. 102, 637 (1997).

[16] Certain commercial equipment or instruments are identified in this document. Such identification does not imply recommendation or endorsement by the National Institute of Standards and Technology, nor does it imply that the products identified are necessarily the best available for the purpose.

[17] D. M. Pease, D. L. Brewe, Z. Tan, and J. I. Budnick, *Phys. Lett. A* 138, 230 (1989).

[18] Y. Suzuki, *Phys. Rev. B* 39, 3393 (1989).

[19] A. I. Frenkel, D. M. Pease, J. I. Budnick, P. Shanthakumar, and T. Huang, *Journal of Synchrotron Radiation* 14, 272 (2007).

[20] R. V. Vedrinskii, V. L. Kraizman, A. A. Novakovich, P. V. Demekhin, and S. V. Urazhdin, *J. Phys.: Condens. Matter* 10, 9561 (1998).

[21] L. V. Azaroff. *Elements of X-Ray Crystallography* (McGraw-Hill, New York, 1968).

[22] J. H. Park, L. H. Tjeng, A. Tanaka, J. W. Allen, C. T. Chen, P. Metcalf, J. M. Honig, F. M. F. de Groot, and G. A. Sawatzky, *Phys. Rev. B* 61, 11506 (2000).

[23] U. von Barth and G. Grossmann, *Solid State Commun.* 32, 645 (1979).

[24] C. Brouder. *J. Phys.: Condens. Matter* 2, 701 (1990).

[25] B. Ravel, E. Stern, R. Vedrinskii, V. Kraizman. *Ferroelectrics* 206, 407 (1998).

[26] B. Ravel, Ph. D. Dissertation University of Washington preprint (unpublished), 1997.

[27] B. Poumellec, V. Kraizman, Y. Aifa, R. Cortès, A. Novakovich, and R. Vedrinskii. *Phys. Rev. B* 58, 6133 (1998).

[28] S. Nozawa, T. Iwazumi, and H. Osawa, *Phys. Rev. B* 72, 121101 (R) (2005).

[29] B. Poumellec, V. Kraizman, Y. Aifa, and R. Cortez, *Phys. Rev. B* 58, 6133 (1998).

[30] J. Wong, F. W. Lytle, R. P. Messmer, and H. W. Maylotte, *Phys. Rev. B* 30, 5596 (1984).

[31] W. Vining, A. Goodrow, J. Strunk, and A. T. Bell, *J. of Catalysis* 270, 163 (2010).